MILLS, K.C., FOX, A.B., THACKRAY, R.P. and LI, Z. The performance and properties of mould fluxes. *VII International Conference on Molten Slags Fluxes and Salts,* The South African Institute of Mining and Metallurgy, 2004.

The performance and properties of mould fluxes

K.C. MILLS, A.B. FOX, R.P. THACKRAY and Z. LI
Department of Materials, Imperial College London, United Kingdom

The role of mould fluxes in continuous casting is reviewed. The main functions of the flux are described and the importance of the flux in providing lubrication and the right level of heat transfer between the shell and the mould is described. The major problems of longitudinal, transverse and star cracking, gas and slag entrapment and deep oscillation marks in the steel product and 'sticker breakouts' are analysed. The important physical properties of the flux in combating these various problems are identified. Physical property data for the fluxes are given.

Introduction

Mould fluxes have a major role in the continuous casting of steel. The powders are fed onto the top of the molten metal surface, whereupon they form first a sinter layer, then a mushy layer, and eventually form a liquid flux pool (Figure 1a). Liquid slag from the molten pool infiltrates into the mould/strand channel and lubricates the newly-formed steel shell. However, most of the first liquid entering the channel freezes against the water-cooled, copper mould and forms a glassy, solid slag film (typically *ca.* 2 mm thick[1]). A thin liquid slag film (*ca.* 0.1 mm thick) moves with the steel shell and provides liquid lubrication to the shell. In time, the glassy slag may partially crystallize. The solid slag layer is usually considered to stay attached to the mould wall or, if it does move, it must be much slower than the velocity of the shell. The mould is oscillated to prevent the shell from sticking to the mould. The horizontal heat transfer is controlled by both the thickness and the nature of the solid slag layer. Thus, in summary, the liquid slag layer controls the lubrication and the solid slag layer controls the horizontal heat transfer.

It is generally accepted that the depth of the molten slag pool (d_{pool}) should exceed the stroke length to ensure good slag infiltration (i.e. lubrication of the steel shell) and frequently a depth of >10 mm[2,3] is recommended. The depth of the molten pool affects both the amount of liquid slag infiltrating into the mould / strand channel[2,3] and the number of inclusions transferred from the steel to the molten slag[4].

The role of the slag in continuous casting is to:

- Protect the meniscus of the steel from oxidation
- Provide thermal insulation to prevent the steel surface from freezing
- Provide liquid slag to lubricate the strand
- Provide the optimum level of horizontal heat transfer for the steel grade being cast
- Absorb inclusions from the steel.

All of these functions are important but in routine practice it is the lubrication and the horizontal heat transfer, that are the most important. The principal factors affecting flux performance are:

- Casting conditions (casting speed, V_c, oscillation characteristics)
- Steel grade and mould dimensions
- Mould level control (which can lead to depressions etc.)
- Metal flow, since turbulent flow can lead to several problems e.g. gas and slag entrapment.

We will see that efficient execution of the tasks listed above requires the optimization of the physical properties of the flux.

Mould fluxes are usually made up of about 70% (CaO and SiO_2), 0–6% MgO, 2–6% Al_2O_3, 2–10% Na2O (+ K_2O), 0–10% F with varying additions of TiO_2, ZrO_2, B_2O_3 Li_2O, and MnO. The basicity, (%CaO / %SiO_2) lies in the range 0.7 to 1.3. Carbon particles in the form of coke breeze, carbon black and graphite are added (2–20%) to (i) control the melting rate and (ii) to form a reducing atmosphere of CO (g) in the upper mould to protect the metal from oxidation. Carbon particles are non-wetting to slag and thus slag globules are prevented from agglomerating by carbon particles until the latter are consumed by oxidation; this is the mechanism for the control of melting rate.

Flux properties and functions of mould flux

Lubrication and powder consumption

The liquid mould flux lubricates the steel strand. It is important that there is liquid lubrication throughout the strand since problems (such as star cracking of the steel) can occur if the flux crystallizes completely in the lower half of the mould and liquid lubrication is lost[5,6]. For the fully liquid flux, assuming Newtonian behaviour the liquid friction (F_l) is given by Equation [1] where V_m is the velocity of the mould, and A is the area of the mould. It can be seen that the friction decreases as the viscosity (η) decreases and the liquid flux film thickness (d_l) increases.

$$F_l = A\eta\ (\ V_m - V_m)\ /\ d_l \qquad [1]$$

Powder consumption, Qs provides a measure of the lubrication supplied and it is very dependent upon mould size since the friction increases as the distance from the corner increases[7] Thus frictional forces are much larger in slabs > blooms > billets and increase with increasing

viscosity of the liquid. Powder consumption (Q_t) is usually measured as kg flux (tonne steel)$^{-1}$. However, Q_t can be converted to Q_s with units of kg flux m^{-2} (of mould) using Equation [2].

$$Q_s = f^*.Q_t.\ 7.6/\ R = d_l\ \rho \quad [2]$$

where f^* is the fraction of powder producing slag, ρ the density of the liquid slag and R is the (surface area to volume ratio of the mould) and is given by 2(w + t)/wt, where w and t are the width and thickness of the mould, respectively. The friction forces increase with increasing distance from the corner so, consequently, more lubrication (i.e. higher Q_s) is required for slabs > blooms > billets.

Inadequate powder consumption has been reported to lead to a variety of defects and problems namely, (i) longitudinal cracking, (ii) sticker breakouts (which are always related to lack of lubrication), (iii) deep oscillation marks, (iv) transverse corner cracking, (v) off-corner cracking, and (vi) the formation of depressions.

The powder consumption is made up of several contributions. Most workers identify two contributions to the powder consumption (i) that used to lubricate the mould, Q_{lub} and (ii) that trapped in the oscillation marks, Q_{om}. Three mathematical models have been reported[8-10] which allow the calculation of Q_{om} but it has been shown recently[11], that they usually overestimate Q_{om} by a considerable amount. Itoyama[17] reported *Qlub* contained contributions from (i) flow emanating from the molten pool (ii) flow between parallel plates (mould and strand), and (iii) arising from the oscillation of the mould. Several empirical rules have been proposed[12–20] for the calculation of Q_s from values for various casting parameters (casting, speed, flux viscosity, etc.). Recently, a statistical analysis of plant data for Q_s showed that the following parameters had statistical significance, slag viscosity, casting speed, oscillation frequency (f) and stroke length and the break (T_{br} see 'Break solidification' below) or solidification temperature (T_{sol})[21]. From the viewpoint of the mould flux, powder consumption increases as the flux viscosity and break temperature both decrease.

The melting rate (M_R) must meet the demand for liquid slag (i.e. the powder consumption). It is controlled primarily by (i) the amount of free carbon and (ii) the particle size of the carbon. The melting rate can be calculated from the following relation[12].

$$\%C_{free} = -0.016M_R + 15.41 \quad [3]$$

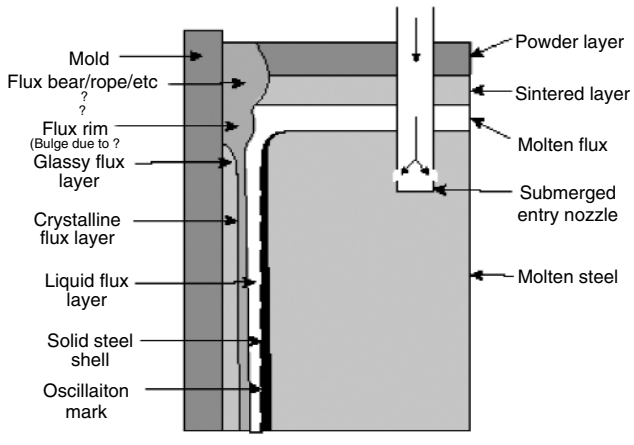

Figure 1. Schematic representation of the various slag layers formed in the mould

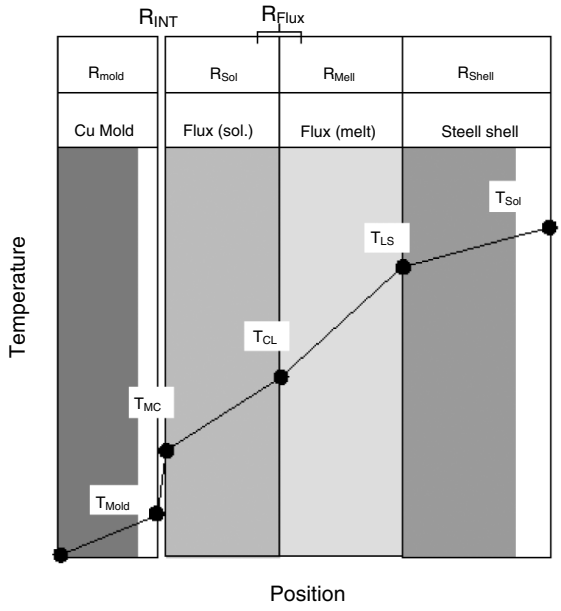

Figure 2. Schematic representation of the thermal resistance affecting horizontal heat transfer between steel shell and mould wall

Horizontal heat flux, q_{hor}

Horizontal heat transfer is a complex process involving two mechanisms, namely, lattice or phonon conductivity (k_c) and radiation conductivity (k_R). Radiation conductivity involves absorption and re-emission of radiated energy and can be the dominant conduction mechanism in glassy materials at high temperatures. The radiation conductivity can be calculated from Equation [4] for optically thick conditions (defined as αd >3) where α = absorption coefficient, d = thickness, σ = Stefan Boltzmann constant, n = refractive index (usually around 1.60), and T is the thermodynamic temperature (K)

$$k_R = 16\sigma n^2 T^3 / 3\alpha \quad [4]$$

However, k_R can be significantly decreased by the presence in the slag film of:

(i) crystallites that scatter the radiation (extinction coefficient $E = \alpha + S$ where S is the scattering coefficient and E should be used for solids)
(ii) transition metal oxides that absorb the radiation e.g. FeO

It has been estimated that k_R = 10–30% kc[22–24] for heat transfer across slag films formed during industrial slab casting. However, it may be much more significant in glassy slag films formed using high-viscosity fluxes for billet casting.

The overall resistance to thermal transfer (R^*total) between shell and mould can be regarded as a series of resistances as shown in Figure 2 and Equation [5].

$$R^*_{total} = R^*_{Cu/sl} + (d/k)_l + (d/k)_{gl} + (d/k)_{cry} \quad [5]$$

where $R^*_{Cu/sl}$ is the interfacial resistance and subscripts l, gl and cry denote the liquid, glass and crystalline layers, respectively. Radiation conductivity can be taken into account as a parallel resistance[24]. The largest terms in Equation [5] affecting (R^*_{total}) are (i) $R^*_{Cu/sl}$ and (ii) the thickness of the solid slag film ie $d_{solid} = d_{gl} + d_{cry}$.

The interfacial resistance $R^*_{Cu/sl}$ was found[25,26] to increase with (i) increasing solid slag thickness, d_{solid} and (ii) increasing crystallinity (Figure 3), and (iii) had values

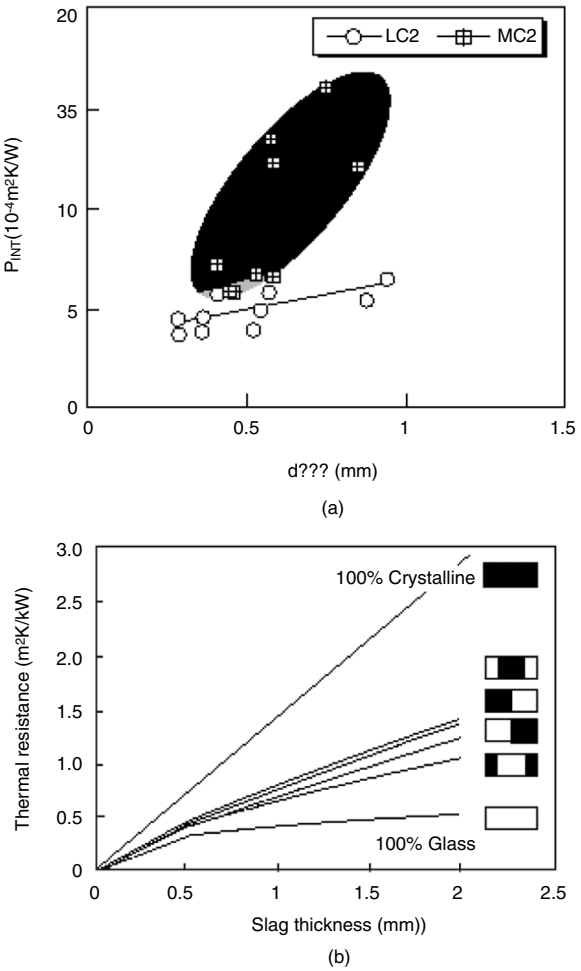

Figure 3. The effect of (a) mould fluxes for the casting of medium (MC) and low (LC) carbon steels[23] and (b) the crystallinity on the interfacial resistance[26]

around 5×10^{-4} m²K W^{-1}. The effect of increasing crystallinity on $R_{Cu/sl}$ is best understood as shrinkage resulting in the formation of an air gap (or surface roughness)[27] when a glass transforms into a more dense, crystalline phase ($\rho_{cry} > \rho_{gl}$).

Thus the two key parameters affecting horizontal heat flux are (i) the thickness of the solid slag film (d_{solid}) and (ii) the % crystalline phase developed in the slag film. Other parameters of interest are the thermal conductivity of the solid and liquid phases and the absorption and extinction coefficients and the refractive index.

Thermal insulation (vertical heat flux)

The powder bed must provide sufficient thermal insulation to prevent the freezing of the steel surface. Reduction of the vertical heat flux (q_{vert}) is also important in the reduction of the depth of the oscillation mark and in reducing' pinholes' by reducing the length of the meniscus hook (Figure 4)[28]. The thermal insulation is dependant upon the nature of the flux bed but, in general, insulation increases:

- in the hierarchy powders > extruded granules > spherical granules
- As the size of the granules is decreased
- As the thickness of the flux bed is increased
- With the introduction of an exothermic agents such Ca/Si.

Absorption of inclusions

The absorption of inclusions by the flux is important since the mechanical properties of the steel are dependent both the number and size of the inclusions present. The absorption process involves several steps (1) transport of inclusion to the slag/metal interface, (2) attainment of the required interfacial requirements for passage to the slag phase (clarity), (3) dissolution of the inclusion by the slag pool, (4). and transport away from the interface.

Inclusion separation from steel to flux is promoted by: (a) a high contact angle between inclusion and metal and slag, (contact angles $\theta = 130°$ for Al_2O_3 and steel and 160° for TiN for a 18/8 stainless /inclusion /slag system have been reported) and (b) wetting of inclusions (most inclusions are wetted by slags)[29].

Dissolution of inclusions in the flux is promoted by high values of (C_{sat}-C) i.e. the difference between saturation concentration and the actual concentration in the slag. Thus dissolution is aided if C_{sat} is high. (C_{sat} has values of *ca.* 40% for Al_2O_3, 10% for TiO_2, 2% for ZrO_2 and 0.5% TiN). Thus problems in casting stainless steels relate to the large amount of undissolved, solid TiN or $CaTiO_3$ in the slag pool which, in turn, increases the viscosity dramatically.

Metal flow turbulence

The metal flow in the mould has a significant effect on the process. Turbulent metal flow can cause the formation of a standing wave (Figure 5): the turbulent flow in the metal causes an associated drag flow in the slag pool and these effects can cause the following problems:

- Slag and gas entrapment causing surface defects in the rolled product
- Carbon pick-up, especially in ultra-low carbon (ULC) grades
- SEN erosion, especially at the metal/ slag interface
- Freezing of the steel surface due to decreased insulation resulting from spherical granules running down the standing wave.

The principal causes of turbulent flow lie in (i) the immersion depth of the submerged entry nozzle (SEN) (ii) the design of the SEN ports, and (iii) Ar flow rate. Despite this, the mould flux is frequently expected to compensate

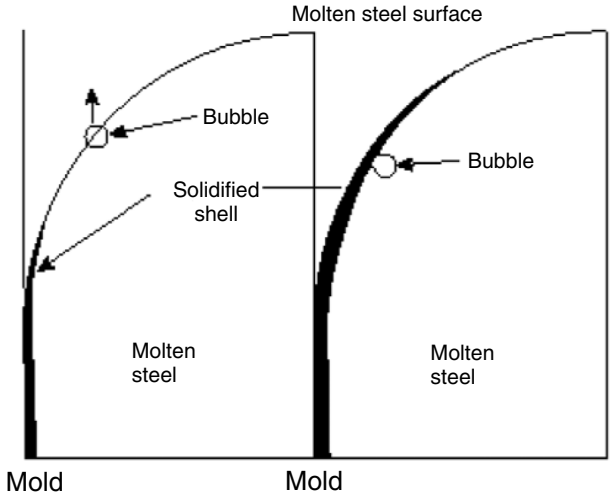

Figure 4. Schematic drawing showing on the right a gas bubble captured by the meniscus, and on the left how the bubble keeps rising when the meniscus length is smaller

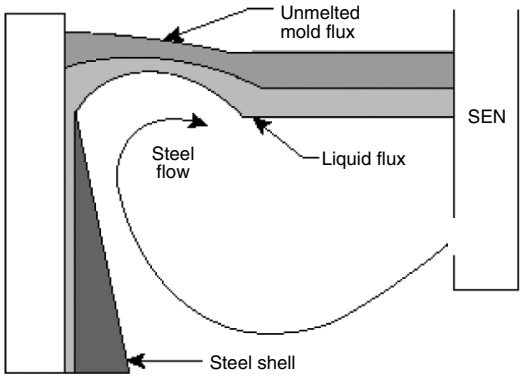

Figure 5. Schematic diagram showing the standing wave formation

for the effects of the turbulent flow, usually by use of a flux with a higher viscosity, but this leads to a reduction in the powder consumption, which can lead to other problems as mentioned above.

Defects and process problems

Longitudinal cracking and longitudinal corner cracking

Longitudinal cracking is a serious problem and is particularly prevalent in medium carbon (MC) steels. The problem arises as a result of the 4% difference in the thermal shrinkage coefficients of the δ-Fe and austenite phases, which gives rise to stresses that are relieved by longitudinal cracking. The stresses can be minimized by keeping the solid steel shell as thin and as uniform as possible while in the mould. This is achieved by reducing the horizontal heat transfer by using a thick slag film with a significant crystalline fraction. The thicker slag film is achieved by using a flux with a high solidification or break temperature.

Sticker breakout

There are probably several causes of sticker breakouts, however, all of them involve a lack of lubrication. High C steels (> 0.4% C) are prone to sticker breakouts due to the low strength of the shell near the meniscus, caused by enhanced micro-segregation of ferrite between the austenite grains.

Sticker breakouts can occur as a consequence of the formation of a pseudo-meniscus, which is formed as a result of a constraint. It has been reported[31] that these sticker breakouts occur as a result of;

(i) a carbonaceous agglomerate being forced to the edge of the mould
(ii) carbon diffusing out of the agglomerate and forming a C-rich, low-melting, shell, which does not completely freeze during healing time (positive strip)
(iii) the agglomerate blocking the local flow of slag into the mould/strand gap.

Several sources of carbon-rich agglomerates have been proposed: (i) unmelted mould powder attached to the slag rim[30], (ii) the carbon-rich layer floating at the top of the slag pool, and (iii) parts of the SEN and stopper rod ripped out by ferrostatic pressure on Al_2O_3 accretions[31].

It is known that glassy slags are beneficial in reducing sticker breakouts. Although sticker breakouts are associated with lack of lubrication, the usual strategy to minimize breakouts is to form a thicker, stronger shell by increasing the horizontal heat flux. This is achieved by using a thin glassy slag layer i.e. the opposite of the procedure used to combat longitudinal cracking. The thin slag film is achieved by using a flux with a low solidification or break temperature.

Oscillation marks and transverse cracking

Oscillation marks are horizontal indentations occurring at regular intervals along the surface of the steel surface and must be removed by grinding (before rolling). There are two types of oscillation marks (OM):

Hook or Overflow type (Figure 6) formed by overflow of liquid steel over the tip of newly-formed shell; the solidified shell grows upward and inward (away from the mould) and molten steel overflows the tip of the shell and a mark is formed.

Depression or folded type is formed by curvature of the shell (as in the hook type) but no overflow takes place and the tip of the shell is bent backwards and grows towards the mould and forms a bay on the surface. Cracks often form in the bottom part of the bay, as a result of micro-segregation. The rim plays an important role because it narrows the entrance to the channel and thus magnifies the pressure variations.

Transverse cracking is related to the formation of deep oscillation marks. The principal factors affecting the depth of oscillation marks, d_{om}, are oscillation characteristics but the pressure in the slag film is an important factor and its relation to slag viscosity has been reported to go through a maximum[3]. Thus careful selection of viscosity may result in decreases in pressure and a reduction in d_{om}. Two other ways of reducing d_{om} involve:

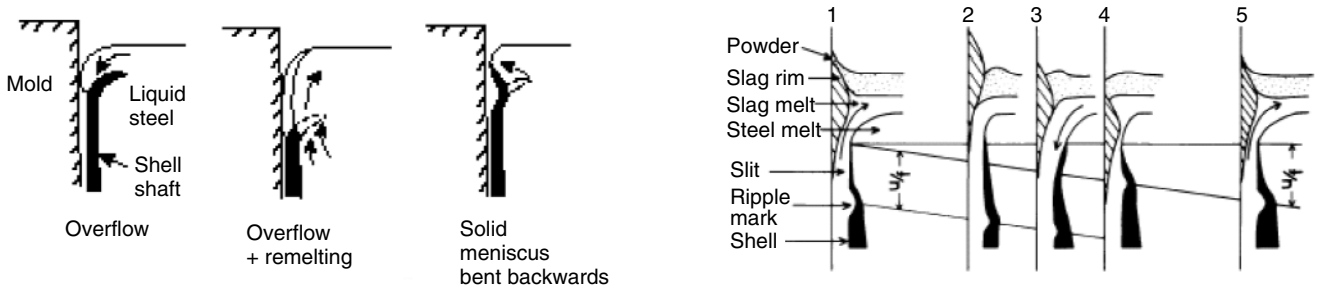

Figure 6. Mechanisms of oscillation mark formation showing on the left hook formation and on the right depression

- decreasing the length of the meniscus tip by reducing the vertical heat flux, and
- increasing the strength of the shell by increasing its thickness through increased horizontal heat flux

Gas and slag entrapment

Gas and slag entrapment is mainly caused by metal flow turbulence[33,34]. An example of slag entrapment is shown in Figure 7. Gas entrapment is similar. The obvious way of combating slag and gas entrapment is to reduce the metal flow turbulence (e.g. adjusting SEN depth and port design, reducing Ar flow, or by reducing the velocity by electro-magnetic braking[35], swirling-flow nozzles[36] or meniscus free casting[37]). In practice, it is often dealt with by increasing the viscosity of the flux but this entails a decrease in powder consumption. It has been pointed out[33] that a more effective way of dealing with slag and gas entrapment is to increase the interfacial tension between the metal and the flux.

Properties of mold fluxes

Viscosity (η)

The viscosity (or fluidity $=1/\eta$) of the mould flux is the most important of the flux properties since:

- It determines the powder consumption and hence the lubrication of the shell
- Slag entrapment is usually dealt with by increasing slag viscosity
- SEN erosion rate is proportional to the fluidity
- It would appear[32,38] that the pressure in the mould/ shell channel, which is related to the depth of the oscillation mark, (d_{om}), goes through a maximum and d_{om} can be minimized by selection of flux viscosity.

The viscosity of the flux is usually cited at 1300°C since this represents the average temperature in the liquid slag layer. Viscosity measurements can be measured reliably to *ca*. ± 10% but errors can be higher in viscometers using graphite components (bobs and crucibles). However, another major source of uncertainty is the *F* losses during the filling of the crucible and the measurement sequence, which can be both significant and dependent upon the procedures used. Few investigators have carried out post-measurement chemical analysis.

Several models are available for the estimation of viscosity from chemical composition[39–42]. A review of the performances[43] of most of these models showed that the Iida model[39] performed best of the models tested on mould fluxes, with an uncertainty of ± 25%.

Break solidification and liquidus temperatures (T_{br}, T_{sol}, T_{liq})

The **liquidus** temperature is the temperature where the flux is completely liquid and is measured on the heating cycle in DTA/DSC runs or Leitz microscope tests. The main importance of T_{liq} is that it determines the interface between the liquid pool and the mushy region in the powder bed. It can be estimated to ±35°C by:

$$T_{liq}\,(°C) = 1191 + 11.4\%SiO_2 - 11.0\%CaO + 4.2\%Al_2O_3 + 5.7\%MgO - 10.1\%Na_2O - 15.8\%K_2O + 1.9\%F + 8.3\%Fe_2O_3 + 11.6\%MnO \quad [6]$$

The **solidification** temperature is the temperature where the molten flux first solidifies (or crystallizes) on cooling; it is usually measured by DTA/DSC or hot thermocouple methods. Kim *et al.*[44] have reported that the solidification temperature can be calculated by the following relation, where x= mole fraction:

$$T_{sol} = 1242°C - 1.4x(Al_2O_3) - 2.1x(MgO) - 4.5x(Na_2O, K_2O) - 8.5x(CaF_2) - 15.3x(B_2O_3) \quad [7]$$

The **break** temperature is the temperature below which there is a marked increase in viscosity as shown in Figure 8a (i.e. the temperature where liquid lubrication starts to break down). In our opinion the liquid in the mould/strand channel behaves similarly to that in a viscometer and for that reason we prefer T_{br} to T_{sol}. In some cases the measured values of T_{br} and T_{sol} are very similar but in other cases there is 70°C difference in the values[44]. The break (and probably solidification) temperatures decrease with increasing cooling rate and are usually measured at –10°C min^{-1} but could be considerably lower in the mould where the cooling rate is **ca**. 10°Cs^{-1}. The break temperature, *Tbr* for a cooling rate of 10°C min^{-1} can be calculated[45] within ±20°C by use of the following relation: for mould slags.

$$T_{br} - 1120°C = -8.43\%Al_2O_3 - 3.3\%SiO_2 + 8.65\%CaO - 13.86\%MgO - 18.4\%Fe_2O_3 - 3.2\%MnO - 2.2\%K_2O - 3.20\%Na_2O - 6.47\%F \quad [8]$$

The break temperature is important because:

- It determines the thickness of the solid layer and therefore affects q_{hor}, and
- It determines the thickness of the liquid layer and thus affects powder consumption and lubrication.

Glassy slags with high viscosity (sometimes used in billet casting) do not exhibit a break temperature but transform gradually from a liquid to a super-cooled liquid until they reach the glass transition temperature (T_g), which usually

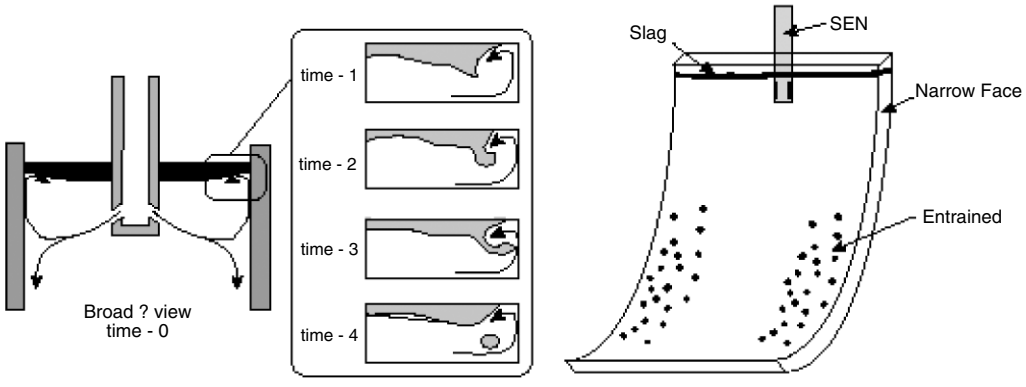

Figure 7. Schematic diagram showing the mechanism of slag entrapment at higher casting speeds

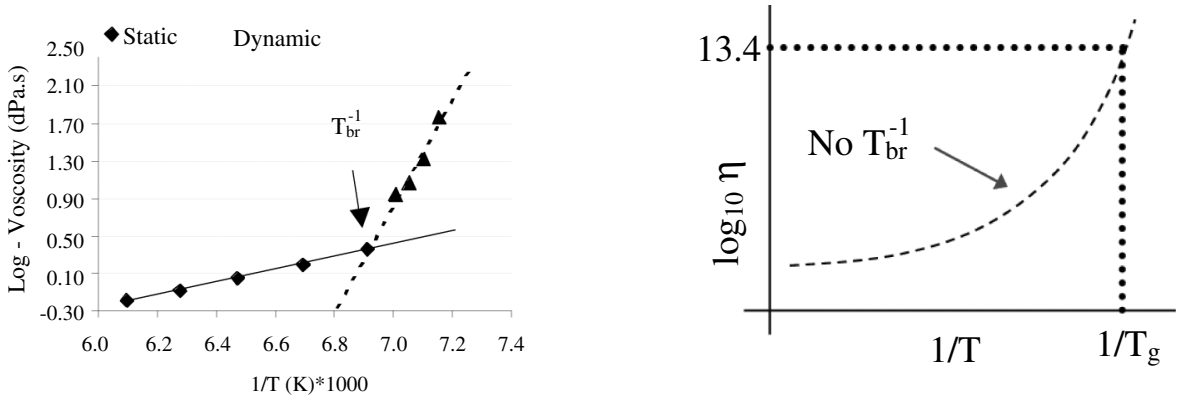

Figure 8. Arrhenius plots showing $\log_{10}$ viscosity (dPa.S) versus reciprocal temperature (K^{-1}) for (a) conventional flux and (b) high viscosity flux for billet casting[12]

occurs around 600°C (Figure 8b). If thermal expansion measurements are performed on a glassy slag it is observed that the sample collapses just above T_g since the super-cooled liquid cannot withstand the pressure of the two probes. It is expected that super-cooled liquids to flow with the shell of the billet and provide some measure of lubrication, despite their high viscosity.

It has been pointed out that the lubrication requirement can be expressed in terms of the viscosity and the horizontal heat flux in terms of the break temperature. Figure 9 shows such a plot where a large amount of plant data for slabs-, bloom- and billet-casting was plotted and it was found that these fell onto three curves[12]:

- MC steels which are prone to longitudinal cracking,
- HC steels which are prone to sticker breakouts, and
- all other grades which fell between these two curves.

Crystalline fraction of the slag film

The thermal resistance $R_{Cu/sl}$ has been found[23] to increase with increases in (i) thickness and (ii) crystalline fraction of the slag film (Figure 2). This is due to the formation of surface roughness on the mould side (equivalent to an air gap) as the glass transforms into a more dense crystalline phase.

The importance of the crystalline fraction of the slag film to the horizontal heat transfer has catalyzed considerable research effort into crystallisation.

Time-temperature-transformation (T-T-T) curves have been studied by several workers using double hot-thermocouple and quenching techniques[46–47]. T-T-T curves determine the amount of crystalline phase formed in a certain time and temperature. A typical example is shown in Figure 10 where it can be seen that for the slag to attain 50% crystalline fraction at 800°C, it will take >300 s.

Rocabois *et al.*[47] studied the theoretical background to crystallization and reported that although T_{nose}= 0.77 T_{liq} is the usually accepted relation for calculating the temperature of the 'nose' in the TFT curve, the constant for mould fluxes had values around 0.86 ± 0.06.

They also concluded that the calculated critical quenching rate (Rc = {T_{nose}- T_{liq} }/t_{nose} where t = time) was useful for classifying crystallization for different compositions but did not provide a quantitative predictions of crystallization[47]. It has always been assumed that the initial solid layer was glassy and that subsequent annealing of this glassy layer would result in crystallization in the hotter regions (on the shell side) of the slag layer. However, recently, this has been attributed to the fact that:

- The slag film can exist for a long time, and even at relatively low temperatures crystalline phases can be formed (see T-T-T diagram)[6]
- Cuspidine has the highest T_{sol} and is first phase formed and is precipitated on mould side and crystallites grow across to the shell side[49]
- The temperature on mould side of the slag film is > 600°C and thus crystallization can take place.

It has been reported that cuspidine ($3CaO.2SiO_2.CaF_2$) is formed in the primary crystallization and nepheline or carnegieite in the secondary phase[47].

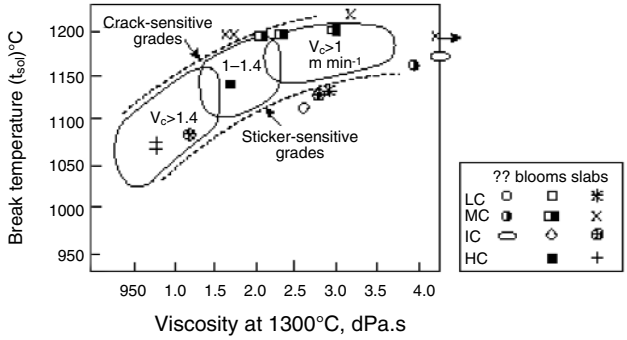

Figure 9. Relation between flux viscosity, break temperature and casting speed[12]

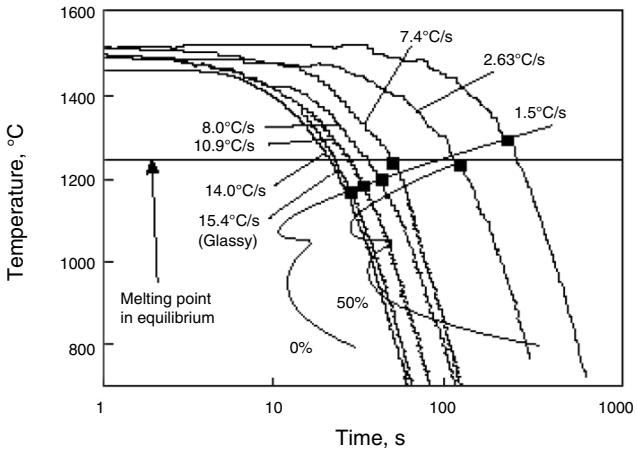

Figure 10. Continuous cooling curves compared with isothermal TTT curves[46]

The amount of crystalline phase present in a slag film has been determined using several methods including optical microscopy, X-ray DTA and DSC methods[50] and measurements of surface roughness[51]. Several tests have been designed to determine the amount of crystalline phase formed in the slag film in a mould flux[52–54].

There is a need to determine the amount of crystallinity developed in a slag film from the chemical composition of the flux. Li *et al*.[54] tried various parameters representing the amount of de-polymerization of the melt as a measure of crystalline fraction. It was found that the modified non-bridging oxygen per tetragonally bonded atom (Si, Al), NBO/T provided a best measure of the crystalline fraction (Figure 11).

$$NBO/T = \frac{2x_{CaO} + 2x_{BaO} + 2x_{CaF_2} + 2x_{Na_2O} - 2x_{Al_2O_3} + 6x_{Fe_2O_3} + (2x_{MgO} + 2x_{MnO})}{x_{SiO_2} + 2x_{Al_2O_3} + x_{TiO_2} + 2x_{B_2O_3} + (x_{MgO} + x_{MnO})} \quad [9]$$

where × = mole fraction of the component in the mould flux. The bracket in the denominator/numerator means it will be included into the denominator if MgO is larger than 7.0% and or MnO is larger than 4.0%, otherwise it will be included in the numerator.

Interfacial tension (γ_{ms})

The interfacial tension is important to the continuous casting process since:

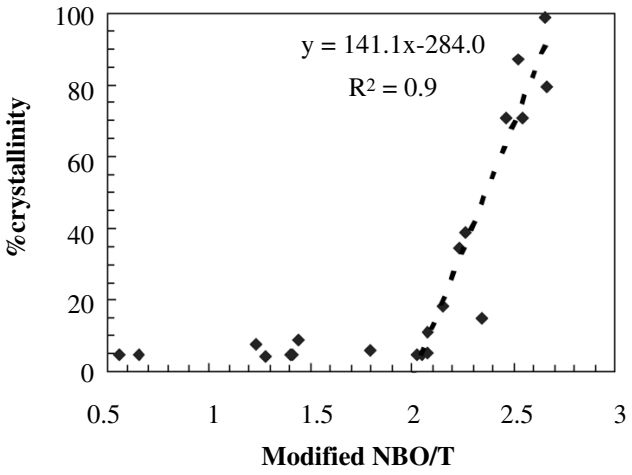

Figure 11. The % crystallinity as a function of the modified NBO/T ratio, which represents depolymerization[54]

- a high gms value helps to minimize slag entrapment
- the shape of the meniscus and hence the width of the channel for slag infiltration is determined by the capillary constant, which involves γ_{ms}[55].

Interfacial tensions are usually measured using the X-ray sessile drop apparatus[56].

Several workers have used fluxes with all Na compounds removed in an attempt to maximize gms in attempt to reduce slag entrapment. Cramb and coworkers[57] report that gms is increased by Al_2O_3, and decreased by Na_2O.

The interfacial tension is given by the relation[56]:

$$\gamma_{ms} = \gamma_{mg} + \gamma_{sg} - \phi(2\gamma_{mg}\gamma_{sg})^{0.5} \quad [10]$$

where the subscripts relate to the phases *m* = metal, *g* = gas, *s* = slag and the term ϕ can be derived from the free energy difference, ΔG. However, it should be noted that the biggest term in the above equation is the surface tension γ_{mg} and this is largely determined by the *S* concentration of the metal. Thus adjustments of the flux composition are less likely to have a large effect on γ_{ms} than adjustments to the *S* concentration of the metal.

Thermal properties

Thermal properties of the slag film obviously play an important part in the horizontal heat transfer between shell and mould. Thermal diffusivity values have been reported by various workers[22,58,59] on glassy, crystalline and liquid slags and on slag films taken from the mould. Some typical values are given in Figure 12. Thermal diffusivity for glassy samples lie between 4 and 5 $\times 10^{-7}$ m^2s^{-1}. We have seen that increasing crystallinity results in a lower heat flux yet, paradoxically, crystalline samples have higher thermal diffusivity values than the glassy samples; this is another consequence of the fact that density of the crystalline phase is greater than that of the glass.

Heat capacity (C_p) and density (ρ) values are needed for calculating conductivity (k) (k = a.C_p. ρ); these can be estimated as functions of temperature (to < ± 5%) from the chemical composition of the slag[60]. Approximate values for these properties are: r = 2600 kg m^{-3} for the liquid phase and C_p values ($JK^{-1}g^{-1}$) of 0.8, 1.1 and 1.43 for 25°C, 600°C and the liquid phase, respectively.

Holzgruber *et al*.[60] carried out simulation experiments of the heat transfer across slag films and derived equations relating the overall thermal conductivity, k_{sys} of the system, as a function of chemical composition of the flux, (in W $m^{-1}K^{-1}$):

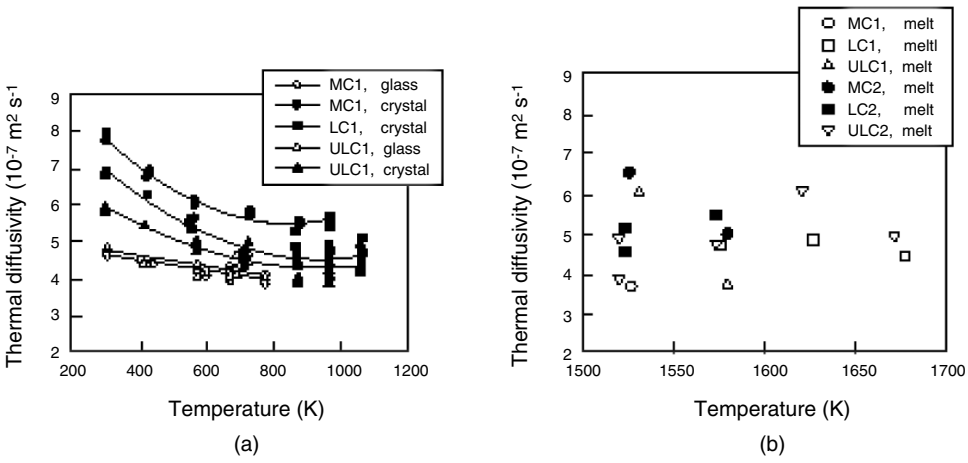

Figure 12. Thermal diffusivities of (a) solid mould fluxes and (b) liquid mould fluxes[58]

$$k_{sys}(1200^{o}C) = 2.03 - 0.459\left[\frac{\%"CaO"}{\%SiO_2} + \%B_2O_3\right] - 0.1695\%FeO - 0.0348\%Al_2O_3 \quad [11]$$

where

$$\%'CaO' = \%CaO + \%MgO + \%MnO + \%Na_2O + \ldots$$

For the optical constants needed to calculate the radiation conductivity (kR) the refractive index (n) has a value of about 1.60 for mould fluxes. Extinction coefficients cannot be predicted but can be measured in transmissivity[62,63] or reflectance[63] experiments. Absorption coefficients (α) for the liquid and glass phases are measured in the same way but are dependent upon the amount of FeO, MnO, Cr_2O_3, NiO present in the flux. Equation [12] provides an empirical rule[62] for calculation of the absorption coefficient.

$$\alpha(m^{-1}) = \alpha^{o} + K\%MO \quad [12]$$

where α^{o} is the absorption coefficient for the slag with 0% transition oxide and K has values of 910, 5 and 410, $m^{-1}\%^{-1}$ respectively for FeO, MnO and NiO. $K(Cr_2O_3)$ was greater than k(FeO).

Where crystalline slag films are formed the absorption coefficient will be much smaller than the scattering coefficient and will not be very influential. However, for high viscosity fluxes used in billet casting, the absorption coefficient will control the radiation conductivity, which could make a significant contribution to the horizontal heat flux in this case.

Effect of chemical composition on individual physical properties

The effect of individual components of mould flux are summarized in Table I.

Conclusions

The physical properties of the mould flux play an important part in successful continuous casting operations. The flux properties having the largest influence on continuous casting performance are the viscosity (on lubrication) and the break temperature (T_{br}) and % crystallinity in the slag film (on the horizontal heat flux). The metal/slag interfacial tension is important in relation to the minimization of the depth of oscillation marks and slag entrapment.

References

1. FONSECA, M.V.A. *et al.*, *5th Intl. Conf. on Molten Slags, Fluxes and Salts*. 1997. Sydney, Australia, p. 851.
2. JENKINS, M.S. 'Heat Transfer in the Continuous Casting Mould', 1999, PhD thesis, Monash Univ., Australia.
3. ITOYAMA, S. *et al.*, Evaluation of Mould Flux Composition in Continuous Casting of Steel based on Cold Mould Experiments, *CAMP - ISIJ*, 2001. vol. 14, p. 893.
4. SCHELLER, P.R. *2nd Intl. Cong. Sc. & Tech. Steelmaking*. (2001), Swansea publ: IOM, London, p. 667.
5. T.J.H. BILLANY, A.S. NORMANTON, K.C. MILLS, and P.GRIEVESON, *Ironmaking and Steelmaking*, vol. 18, 1991, p. 403.
6. O'MALLEY, R.J. and NEAL, J. *Proc. Intl. Conf. New Developments in Metall. Proc. Technol.*, 1999, Dusseldorf: METEC Congress, p. 73.
7. OGIBAYASHI, S. *Intl. Workshop on Thermophys. Data for the Development of Math. Models of Solidification*, held Gifu City, Japan, 1995.
8. ITOYAMA, S. *et al, CAMP-ISIJ*, vol. 14, 2001, p. 893.
9. T. Y. MENG and B. THOMAS, *Proc. ISS Tech 2003*, held Indianapolis, IN, publ ISS, Warrendale, PA, 2003.
10. Y. ITOH, S. NABESHIMA, and K. SORIMACHI, *Proc. 6th Intl. Conf on Molten Slags, Fluxes, and Salts*, held Stockholm, Sweden, 2000.
11. SARASWAT, R. *unpublished results*, 2003.
12. FOX, A.B. Ph.D. thesis, 2004, University of London.
13. KWON, O.D. and CHOI, J. *et al*, in *ISS Steelmaking Conference*. 1991, ISS Warrendale, PA, p. 561.
14. MAEDA, H. and HIROSE, T. *et al*, *CAMP - ISIJ*, vol. 6, (1993), p. 280.
15. NAKAJIMA, K. *et al.*, *CAMP - ISIJ*, vol. 5, 1992, p.1221.
16. LUDLOW, V. *et al.* Final Report EUR 18371 EN, ECSC Contract No., 7210.CA/838/430/433, 2000.
17. WOLF, M. *Proc. of Continuous Casting of Steel in the Developing Countries*. 1993, Beijing, China, p. 66.
18. TSUTSUMI, K. *Tetsu-to-Hagané*, vol. 84, no. 9, 1998, p. 617.
19. T. KITAGAWA and M. ISHIGURO, in *4th Japan-Germany Seminar Proc*. (1980): ISIJ, p. 249.
20. Y. KOBAYASHI and S. MARUHASHI, in *4th Japan-CSSR Seminar*, (1983), Ostrava, p. 249.
21. R. SARASWAT, *Scand. J. Metall*, in press
22. R. TAYLOR and K.C. MILLS, *Ironmaking and Steelmaking*, vol. 15 1988, p.187.
23. CHO, J.W., EMI, T., SHIBATA, H., and SUZUKI, M. *ISIJ Intl*, vol. 38, 1998, p. 844.
24. YAMAUCHI, A. 'Heat transfer phenomena and mould flux lubrication in continuous casting of steel', Ph.D. thesis, 2001, KTH, Stockholm.
25. WATANABE, K. *et al.*, *Proc. of Steelmaking Conf*, 1996, p. 265.
26. JENKINS, M.S. Ph.D. thesis, 'Heat transfer in the continuous casting mould', 1999, Monash University, Australia.
27. TSUTSUMI, K. *et al, ISIJ Intl*, vol. 39, 1999, p. 1050.
28. NEUMANN, F. *et al., Steelmaking Conf. Proc.*, 79, Warrendale, Pa; Iron and Steel Society 1996, p. 86.

Table I
Summary of the effects of different components on mould flux properties

Property /Constituent	CaO	SiO_2	Al_2O_3	MgO	$Na_2O + K_2O$	FeO_x	CaF_2	MnO	B_2O_3	ZrO_2
Viscosity	↓	↑	↑	↓	↓	↓	↓	↓	↓	↔
T_{br}	↑	↓	↓	↓	↓	↓	↓	↓	↓	↑
T_{sol}	↑	↓	↓	↑	↓		↓	↓	↓	↑
γ_{ms}	↑	↓	↑			↓		↓		
Thermal cond (k) Diffusivity(a)	↓	↑	↑	↓						
Crystall'n Tendency	↑	↓	↓	↓[a]	↓[a]		↑	↓	↓	↑

[a] above about 5 %

29. SHARAM, H. and CRAMB, A.W. *ISS Trans*, vol. 15, 1995, p. 95.

30. MUKAI, M. *et al, Trans ISIJ,* vol. 26, no. 4 1986. p. B163.

31. MILLS, K.C. and BILLANY, T.H. *Ironmaking and Steelmaking*, vol. 18 1991, p. 258.

32. JENKINS, M.S. and MAHAPATRA, C.B. *6th Conf of Asia Pacific Confed. Chem. Eng*., 3, Melbourne, 1993, p. 311.

33. FELDBAUER, S. and CRAMB, A.W. *Proc. Steelmaking Conf*, 78, Nashville, TN, Warrendale, Pa, Iron and Steel Society, 1995.

34. NAKATO, H. *et al., Continuous casting*, vol. 6 Warrendale, Pa, Iron and Steel Society, p. 193.

35. TANI, M. *et al., Proc 4th Europ. Conf. Cont. Casting,* Birmingham, UK, 2002, IOM, London 2002.

36. YOKOYA, S. *et al., Proc 4th Europ. Conf. Cont. Casting*, Birmingham, UK, 2002, IOM, London 2002.

37. COURBE, P., LE PAPILLON, Y., and NAVEAU, P. Influence of solidification phenomena on quality aspects of CC semi products, *Proc. ECSC Workshop*, Luxembourg, 2002.

38. SCHWERDTFEGER, K. and SHA, H. *Metall. Trans*. B, vol. 1B, 2000, p. 813.

39. IIDA, T., SAKAI, N., KITA, Y., and MURUKAMI, K. *J.High Temp Soc*, vol. 25, no. 3 1999, p. 93.

40. RIBOUD, P.V. and LARRECQ, M. *Proc. Nat. Open Hearth and Basic Oxygen Conf*., Detroit, MI, 1979.

41. GUPTA, V.K., SINHA, S.P., and RAJ, B. *Steel India*, vol. 21, no. 1, 1998, p. 22.

42. MILLS, K.C. and SRIDHAR, S. *Iron and Steelmaking*, vol. 26, 1999, p. 262.

43. MILLS, K.C. *et al.,* Round robin project on the estimation of slag viscosities, *Scan. J. Metall*, vol. 30, 2001, p. 396.

44. KIM, J.W. *et al., Proc. 4th Intl. Conf. On Molten Slags and Fluxes*, 1997, Sendai, Japan: ISIJ, p. 468.

45. SRIDHAR, S. *et al., Ironmaking and Steelmaking*, vol. 27, 2000, p. 239.

46. ORRLING, C., CRAMB, A.W., TILLANDER, A., and KASHIWAYA, Y. *Iron and Steelmaker*, vol. 27, no. 1 2000, p. 53.

47. ROCABOIS, P. *et al., Proc. 6th Intl. Conf. Metall. Slags and Fluxes*, Stockholm, 2000.

48. BEZZERA, C. *et al., Proc. Mills Symposium*, London, 2002, p. 293.

49. HANAO, M. Mould fluxes for continuous casting, *Tetsu-tu-Hagané*, 2002, pp. 23–-28.

50. MILLS, K.C. *et al., Thermochimica*, vol. 391, 2002, p. 175.

51. WATANABE, K. *Tetsu-tu-Hagané*, vol. 83, no. 2, 1997, p. 115.

52. CHANG, S. *et al., Proc. of Continuous Casting of Steel in Developing Countries*, Beijing, China, 1993, p. 832.

53. SAKAI, H. *Proceedings of 5th International Conference Molten Slags, Fluxes and Salts* 1997, Sydney, ISS, p. 787.

54. LI, Z., THACKRAY, R.P., and MILLS, K.C. *Proc. 7th Intl. Conf. on Molten Slags, Fluxes, and Salts*, Jan 2004, Cape Town, SA.

55. FREDRIKSSON, H. and ELFSBERG, J. *Scan. J. Metall*, vol. 31, 2002, p. 297.

56. CHUNG, Y. Ph.D. thesis, Carnegie Mellon Univ., 1998

57. CRAMB, A.W. *et al., Proc. 5th Intl. Conf on Molten Slags, Fluxes and Salts* (Sydney, Australia, 1997, p. 35

58. SHIBATA, H. *et al., Proc. 5th Intl. Conf. Molten Slags, Fluxes and Salts*, Sydney, Australia, 1997, p. 771.

59. OHTA *et al., Proc. 4th Intl. Conf. on Metall. Slags and Fluxes*, Sendai, Japan, 1997,*ISIJ*, p. 415.

60. MILLS, K.C. and KEENE, B.J. *Intl. Mats. Rev*., vol. 32, 1987, p. 1.

61. HOLZHAUSER, J.F., SPITZER, K.H., and SCHWERDTFEGER, K. *Steel Research*, vol. 70, 1999, p. 252.

62. SUSA, M. *et al, Ironmaking and Steelmaking*, vol. 21, 1994, p. 279.

63. MILLS, K.C. and SRIDHAR, S. *Iron and Steelmaking*, vol. 26, 1999, p. 262.

64. W CHO, J., SHIBATA, H., EMI, T., and SUZUKI, M. *ISIJ Intl*, vol. 38, 1998, p. 268.